

# CODAG: Characterizing and Optimizing Decompression Algorithms for GPUs

Jeongmin Park  
*UIUC*

jpark346@illinois.edu

Zaid Qureshi  
*UIUC*

zaidq2@illinois.edu

Vikram Sharma Mailthody  
*UIUC*

vsm2@illinois.edu

Andrew Gacek  
*UIUC*

andrewg3@illinois.edu

Shunfan Shao  
*UIUC*

shunfan2@illinois.edu

Mohammad AlMasri  
*UIUC*

almasri3@illinois.edu

Isaac Gelado  
*NVIDIA*

igelado@nvidia.com

Jinjun Xiong  
*University at Buffalo*

jinjun@buffalo.edu

Chris J Newburn  
*NVIDIA*

cnewburn@nvidia.com

I-hsin Chung  
*IBM Research*

ihchung@us.ibm.com

Michael Garland  
*NVIDIA*

mgarland@nvidia.com

Nikolay Sakharnykh  
*NVIDIA*

nsakharnykh@nvidia.com

Wen-mei Hwu  
*UIUC / NVIDIA*

w-hwu@illinois.edu

**Abstract**—Data compression and decompression have become vital components of big-data applications to manage the exponential growth in the amount of data collected and stored. Furthermore, big-data applications have increasingly adopted GPUs due to their high compute throughput and memory bandwidth. Prior works presume that decompression is memory-bound and have dedicated most of the GPU’s threads to data movement and adopted complex software techniques to hide memory latency for reading compressed data and writing uncompressed data. This paper shows that these techniques lead to poor GPU resource utilization as most threads end up waiting for the few decoding threads, exposing compute and synchronization latencies.

Based on this observation, we propose CODAG, a novel and simple kernel architecture for high throughput decompression on GPUs. CODAG eliminates the use of specialized groups of threads, frees up compute resources to increase the number of parallel decompression streams, and leverages the ample compute activities and the GPU’s hardware scheduler to tolerate synchronization, compute, and memory latencies. Furthermore, CODAG provides a framework for users to easily incorporate new decompression algorithms without being burdened with implementing complex optimizations to hide memory latency. We validate our proposed architecture with three different encoding techniques, RLE v1, RLE v2, and Deflate, and a wide range of large datasets from different domains. We show that CODAG provides 13.46 $\times$ , 5.69 $\times$ , and 1.18 $\times$  speed up for RLE v1, RLE v2, and Deflate, respectively, when compared to the state-of-the-art decompressors from NVIDIA RAPIDS.

## I. INTRODUCTION

Compression has become a vital component of the data storage infrastructure due to unprecedented data size growth in big-data, high-performance computing (HPC), and data analytics applications [1]–[6]. Compression aims to reduce the number of bits used to represent the data through various encoding techniques specialized for different data types and patterns. Compressed data must be first decompressed before it can be processed by compute operations.

As GPUs are increasingly used to meet the compute throughput demands of emerging big-data workloads [7]–[9],

data analytics pipelines typically read compressed data from the storage devices into the GPU memory and deploy one or more GPU kernels for decompression before performing query computation on the data. Prior works [6], [10] have shown this approach’s benefits over storing and moving uncompressed data. Thus, high-throughput decompression on the GPU is becoming a key requirement to avoid performance bottlenecks in these pipelines. Our profiling of data-dependent queries with the state-of-the-art GPU-enabled RAPIDS pipeline [1], e.g., “What is the average fare per trip for ride starting from Williamsburg?” on the NYC taxicab dataset [11], a popular dataset for evaluating data analytics pipelines, shows that approximately 91% of the total GPU execution time is consumed by the decompression kernel.

Prior works [12]–[14] have proposed various data-layout transformations on compressed datasets to reduce the GPU execution time spent on decompression. However, applying data-layout transformations on existing massive datasets of modern big-data applications [2], [10], [15]–[17] is an expensive proposition, making decompression techniques that require such transformations impractical. Therefore, it’s much more desirable for a decompression scheme to support the standard compressed data formats, e.g., ORC [2], and not require data-layout transformations, a design goal that we aim to achieve in this work.

To better understand why decompression accounts for so much of the GPU execution time, we performed a detailed profiling study of the state-of-the-art GPU decompressor in RAPIDS. As modern compression schemes support indexed access to multiple chunks of compressed data that correspond to fixed-size chunks of uncompressed input data, the state-of-the-art decompressor exploits chunk-level parallelism by assigning compressed chunks to thread blocks. However, data dependencies still serialize the decoding operations within each chunk. Thus, the state-of-the-art decompressor dedicates a single thread, the leader thread, in each thread block to

decode the compressed data and broadcast the decoded information to the remaining threads in the thread block. All threads then collaborate to execute the memory writing or copying operations based on the decoded information. The state-of-the-art decompressor further enhances the memory bandwidth utilization and hides more of the memory latency by dedicating one warp in each thread block to prefetch compressed data.

By profiling the RAPIDS decompressor, we observe that (1) the memory-bandwidth-driven resource provisioning strategy in the state-of-the-art decompressor in fact fails to effectively hide compute operation, memory, and synchronization latencies; and (2) the root cause of the exposed latencies is the insufficient number of decoding (leader) threads that cannot take full advantage of the GPU’s parallelism and provide the GPU warp schedulers with sufficient numbers of concurrently available instructions to hide latencies.

Based on these key observations, we propose CODAG, a modular and flexible framework for high-throughput decompression on GPUs. In CODAG, we assign compressed chunks to warps rather than thread blocks to drastically increase the exploitation of the GPU’s parallelism to process more chunks at any given time, while maintaining the ability to exploit fine-grained parallelism within each chunk. We refer to the assignment of each chunk to a warp as *warp-level decompression*. We believe that the warp-level decompression offers a number of benefits in CODAG. First, warp-level decompression results in a much higher number of active decoding threads, which helps the hardware scheduler to effectively hide memory, synchronization, and decoding compute operation latencies. Second, since warp-level synchronization primitives have much lower latency and higher throughput than block-level synchronization, warp-level decompression reduces synchronization overhead.

On top of that, we further propose (1) a novel strategy for CODAG to ensure that all on-demand reads or writes in each warp are performed on a cache-line granularity and are thus coalesced, making efficient use of the available GPU memory bandwidth; (2) a clean abstraction for common operations during decompression with the associated Application Programming Interface (API) functions as implemented in decompression kernels. This new abstraction provides the flexibility for programmers to easily incorporate their own encoding techniques into the decoding section of the CODAG kernels while leveraging the rest of the kernel to achieve the desired level of latency tolerance and memory bandwidth efficiency.

We make the following key contributions in this paper.

- We conduct a systematic characterization study on the state-of-the-art GPU decompressor, identify the performance bottlenecks, and determine that decompression on modern GPUs is a compute-bound process.
- We present CODAG, a novel and superior GPU resource provisioning strategy for decompressors with various optimization techniques and abstraction. The proposed APIs can support common decompression operations so that

users can easily integrate their compression algorithms into CODAG with low programming effort.

- We demonstrate CODAG’s effectiveness and flexibility by implementing three encoding techniques, i.e., RLE v1, RLE v2, and Deflate. Results based on the NVIDIA A100 GPUs show that CODAG achieves  $13.46\times$ ,  $5.69\times$ , and  $1.18\times$  speedups over a state-of-the-art decompressor, respectively.

## II. BACKGROUND

In this section, we provide an overview of common compression encoding techniques and how their decompression algorithms have been traditionally parallelized. We then briefly explain why the resource provisioning strategies used in the state-of-the-art GPU decompressors limit the performance and efficiency of decompression on GPUs.

### A. Traditional Encoding Techniques

Generally, compressors take a contiguous sequence of bytes and attempt to encode that sequence in as few symbols as possible. The primary measure of merit of a compressor is the ratio of the size of the uncompressed data over that of the compressed data, referred to as the compression ratio. To maximize compression ratio, compressors use an arsenal of encoding techniques each of which targets different data types and patterns. Here, we describe some of the most common encoding techniques.

The run-length encoding (RLE) technique takes advantage of the same byte or value being repeated in a contiguous sequence, called a *run*. The RLE v1 encoding scheme encodes each *run* with two values: a literal and the length of the run.

Delta encoding provides a high compression ratio when there is a contiguous sequence of values and the differences (deltas) between adjacent values are small. Delta encoding stores the starting value and the number of values in the sequence followed by the deltas to create a compressed data representation. The RLE v2 encoding scheme leverages delta encoding in addition to RLE to capture more data patterns and further improve the compression ratio over RLE v1.

Dictionary-based encoding generates compact encoding when sequences of values are repeated between different sections of the uncompressed data. Given a sequence of bytes, the decompressor can use a dictionary to look up the sequence to see if it has been encountered in the past. If so, the repeated instance can be encoded with 2 values, an offset into the dictionary, and the length of the repeated sequence.

In dictionary encoding, some sequences are repeated more than others. Thus, some references (offset/length pairs) appear more frequently than others [18] in the compressed stream. The Deflate encoding scheme sorts the literals and the length-offset pairs according to their frequency into a Huffman tree [19] so that the number of bits used for each is inversely proportional to their frequency, thus minimizing the total number of bits used.

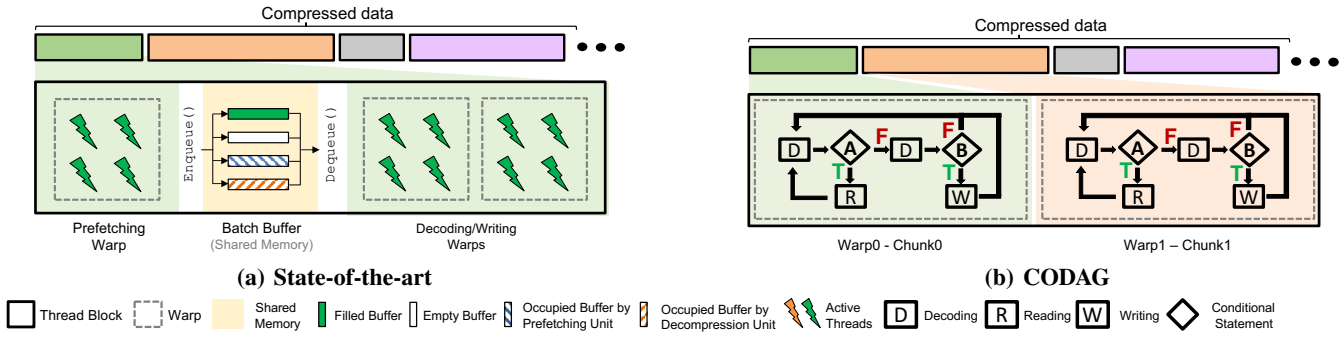


**Fig. 1: Comparison of CODAG with the state-of-the-art decompressor NVIDIA RAPIDS implementation. In CODAG design, the conditional statement A checks whether there is enough space in the input buffer to store full cacheline data, and B checks whether threads need to write uncompressed data based on the decoded information.**

### B. Parallelizing Decompression

Designing high-throughput parallelizable decompression schemes is challenging due to the nature of compressed data. First, compressors output a sequence of variable-length blocks of compressed data, often without any alignment guarantees (See § II-A), resulting in size irregularities. Second, the encoding of a bit or byte in a compressed stream depends on the actions taken for the bits or bytes before it in the stream, creating data-dependencies in the compressed stream. Thus, decompression requires starting at the first byte of the compressed stream and decoding the stream sequentially, limiting parallelism during decompression.

To expose data parallelism during decompression, modern compression data formats divide the uncompressed input into fixed-size chunks, compress each chunk independently, and keep the bytes of the compressed chunk sequential in memory [1], [2], [16]. During decompression, each compressed chunk is assigned to a processing unit so that it can be decompressed independently of other chunks. The data format further specifies metadata for offsets in the uncompressed and/or compressed streams.

### C. State of the Art in Exploiting GPUs for Decompression

As GPUs become increasingly adopted by big-data applications due to their high compute throughput and memory bandwidth, there has been growing interest in high-performance decompression on GPUs. Generally, high-performance decompressors on GPUs assume modern data formats that support chunking. Let’s take a look at how the decompression kernel is mapped to GPU resources in the state-of-the-art NVIDIA RAPIDS implementation [1], [4], [5].

As shown in Figure 1a, after finding the offset for each compressed chunk, RAPIDS assigns each compressed chunk to a thread block, referred to as a decompression unit. Each decompression unit consists of a prefetching warp, batch buffers in the fast shared memory, and decoding/writing warps. RAPIDS opts to use a specialized prefetching warp that fetches bytes of the compressed stream from the slow global memory in a coalesced manner to the batch buffers. Having a specialized prefetching warp in the same thread block as the decoding/writing warps has the benefit of allowing the

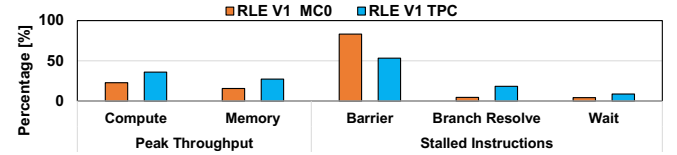


**Fig. 2: The peak throughput percentages and the stalled instruction distribution of RAPIDS decompressor for RLE v1.**

batch buffers to reside in the fast shared memory and the prefetch operations to overlap with the decoding operations for the same chunk. Both features help to reduce the latency of decompressing each chunk.

In the decoding warp, a leader thread is responsible for decoding the bytes from the compressed stream, as this is a sequential process. During decoding, the leader thread reads the data from the batch buffers. When the information has been decoded, the leader thread synchronizes with the other threads in the thread block and directs them to collectively perform a writing operation to the output decompressed data stream in a coalesced manner.

### III. CHARACTERIZATION STUDY OF STATE-OF-THE-ART DECOMPRESSOR

Understanding and optimizing decompression on GPUs is essential as the decompression can consume approximately 91% of total GPU time on a modern data analytics pipeline. However, none of the prior works have performed a detailed analysis of existing state-of-the-art decompression schemes on GPUs. To this end, we conduct an in-depth characterization study of the state-of-the-art decompressor in NVIDIA RAPIDS [1], and identify its key performance bottlenecks.

**Setup:** We use a variety of datasets across different domains as shown in Table IV and evaluate RAPIDS’s decompressor with RLE v1 and Deflate schemes. Due to space limitations, we only present the results from two datasets (MC0 and TPC) but similar trends are observed for the rest. To characterize decompressor performance, we use the system configuration described in Table III and use the NVIDIA Nsight profiling tools to capture important metrics.

**Key insights:** From the left side of Figure 2, we know that for the RLE v1 encoding scheme, both compute and memory resources are far from being fully utilized. As we

discussed in §II-C, these results point to latency exposed due to insufficient parallelism during the decoding process as all threads in a thread block wait on a barrier for the leader thread to complete its decoding operation. To understand the impact of the barrier, we measured the distribution of conditions causing an SM scheduler stall cycle, which is shown on the right side of Figure 2. This metric provides the percentage of threads waiting for each type of stalling condition during the cycles where an SM scheduler cannot find a warp ready for execution.

From Figure 2, during the SM scheduler stall cycles, most (up to 80%) of the threads are not ready because they are waiting on a barrier for the leader thread to complete its current decoding operation. Apart from barriers, up to 20% of the instructions are waiting for the resolution of branch conditions (Branch Resolve) when there is a lack of ready threads for the SM scheduler to dispatch for execution. The Wait metric indicates that a warp is stalled waiting on a fixed latency (arithmetic/logic unit) execution dependency. Moreover, some threads do not receive any work during the writing stage as run lengths can be smaller than the size of the thread block, further degrading the achievable performance.

For Deflate, unlike the traditional view that it is memory bandwidth bound [1], [13], our profiling results in Figure 3 show that its memory bandwidth utilization is less than 25%, which indicates that it is not limited by memory bandwidth but is compute limited. In contrast to RLE v1, Deflate has a much higher utilization of compute throughput (up to 65%) than RLE v1 because of its high computational complexity in dictionary look-up and Huffman tree traversal. We need more detailed metrics and analysis in order to discern whether the performance is limited by a particular type of compute pipeline, memory latency, or compute latency.

We use the profiler to analyze the utilization of the different GPU compute pipelines for Deflate decompression. The right side of Figure 3 shows that the arithmetic logic units (ALU) are up to 55% utilized while the fused multiply/add and load-store units are up to 35% and 20% utilized. This modestly high degree of ALU and FMA utilization mainly comes from the fact that during decoding, the leader thread executes a large number of arithmetic instructions for every byte to identify the next action for generating the output for the byte.

Nevertheless, all these results point to memory latency and/or compute latency as the main limiter of Deflate performance. Due to the high computational complexity of Deflate decoding process, it takes a long time for the leader thread to complete the decoding of each byte while most threads in the thread block are waiting for the decoding thread. During this time, there are not enough decoding threads for the SM scheduler to tolerate the compute pipeline latency. As a result, the execution speed of Deflate is limited by compute pipeline latency in addition to barrier stalling.

**Summary and take-aways:** From the profiling results, we see that the decompression speed of RLE v1 is limited by barrier latency and that Deflate is limited by barrier stall latency as well as the fixed latency of compute pipelines.

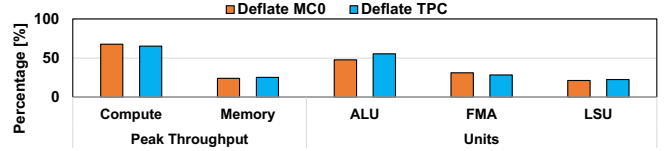


Fig. 3: The compute/memory peak throughput percentages and compute unit utilization of RAPIDS decompressor for Deflate.

Neither the large number of writing threads nor the specialized prefetching warps help address this limitation. Any further improvement in decompression speed for both RLE v1 and Deflate would require more simultaneously running decoding threads (more chunks being decoded in parallel), which is an important design goal of the CODAG architecture.

#### IV. CODAG DESIGN

The goal of CODAG is to provide a flexible framework for high-throughput decompression on GPUs without requiring developers to implement sophisticated, GPU-specific optimizations. CODAG’s architecture, resource provisioning strategy, and kernel APIs enable developers to easily incorporate their encoding techniques of choice into CODAG and rely on the rest of the framework to achieve high decompression speed. On the one hand, as discussed in Section III, the key to improved decompression speed is to increase the number of simultaneously running decompression threads so that the SM scheduler can better hide the synchronization/memory/compute-pipeline overheads.

On the other hand, it is also critical to maintain the coalesced access patterns in reading uncompressed data, reading dictionary value sequences, and writing decompressed data so that the memory access cost does not become excessive and creates new bottlenecks. Thus, the CODAG architecture must address three key challenges in providing an efficient and effective solution that can be used with a wide variety of encoding techniques:

- CODAG must provision GPU execution resources so that many threads can simultaneously decode more chunks in each SM to effectively tolerate latencies and efficiently utilize hardware resources.
- As the naïve on-demand reading and writing operations can make poor use of memory bandwidth and exhibit excessive latency, CODAG must optimally coalesce these accesses to minimize memory access overhead in spite of the irregular consumption of compressed data and sporadic generation of decompressed data by the decoder.
- As the sophisticated optimizations for efficiently using memory bandwidth and tolerating latencies require significant programming skills and efforts, the optimizations in the CODAG framework must be generalized into reusable primitives for a wide range of encoding techniques.

##### A. CODAG System Overview and Abstraction

Figure 1b shows an overview of the CODAG framework. CODAG uses warps as decompression units instead of the larger thread blocks used by the state-of-the-art decompressor, enabling CODAG to simultaneously decompress many

compressed chunks. This enables the hardware scheduler to overlap instruction execution from several independent warps and efficiently hide compute pipeline and memory latencies. In CODAG, all threads in each warp perform the decoding operations as well as amalgamate to read uncompressed data and write decompressed data. Thus, CODAG avoids the high barrier-synchronization overhead that the state-of-the-art decompressor incurs.

In CODAG, each warp executes a decompression GPU kernel that implements a control flow of three main operations: sequential decoding, coalesced reading, and coalesced writing, as shown in Figure 1b. All threads in a warp follow the same control flow to avoid using any broadcast synchronization operations. The control flow consists of a main loop for the decoding process and two conditional statements for on-demand reading and writing operations. During decoding, all threads sequentially execute the same decoding process in compliance with the serial nature of the compressed data stream. In our current framework implementation, the sequential decoding code for different combinations of pertinent encoding techniques can be easily incorporated into the kernel as a CUDA device function.

For coalesced on-demand reading operations, all threads in the warp collaborate to fetch the next cache-line section (e.g., 128 bytes in the A100 GPUs) of the compressed input data stream in a coalesced manner into an input buffer. Having a buffer for the fetched bytes minimizes the number of fetches in spite of the potentially irregular patterns of compressed data consumption during decoding, which helps to reduce the cost of accessing the compressed data. In comparison with the RAPIDS decompressor, CODAG does not have a specialized prefetch warp in each thread block to asynchronously prefetch input data while the thread block’s leader thread is decoding. However, with many independent warps being simultaneously executed, CODAG can still tolerate the memory latency.

When a writing operation is required during decoding, all threads in the warp collaborate to execute the coalesced on-demand writing of a cache-line of the uncompressed output data to the output buffer. Compared to the RAPIDS decompressor, this design at first glance may not seem to offer as much memory parallelism when writing into each output chunk, as RAPIDS uses thread blocks with up to 1024 threads available for writing into each output chunk.

However, the benefit with CODAG is that warp-level barriers are significantly less expensive than their block-level counterparts. Furthermore, with the same thread block size, CODAG supports decompressing and writing up to  $32\times$  more independent chunks in parallel. The increased data parallelism can easily compensate for the loss of memory-level parallelism within a chunk.

As the reading pattern is the same across all encoding techniques, the on-demand reading operation code is portable to all (combinations of) encoding techniques. However, the on-demand writing operations can vary depending on the encoding techniques and need to be specialized by decompressor developers. To shield the decompressor developers

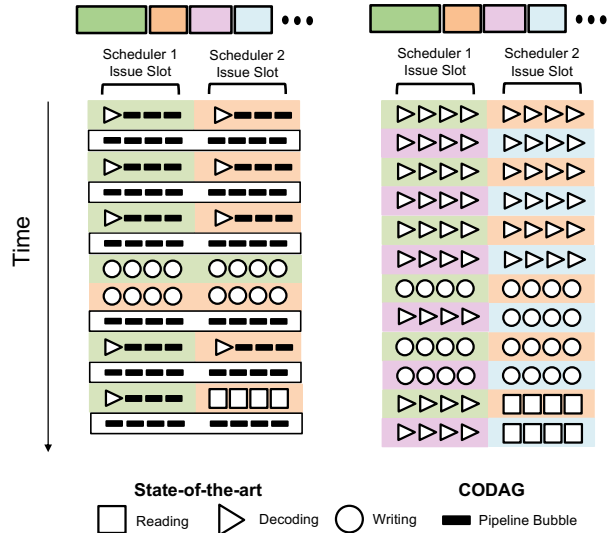


Fig. 4: Illustration of the issued instructions between the baseline and CODAG in a steady state.

TABLE I: CODAG APIs for `input_stream`.

Member Functions	Description
<code>fetch_bits(int n)</code>	Fetch the next $n$ bits in the compressed stream.
<code>peek_bits(int n)</code>	Peek at the next $n$ bits in the compressed stream.

from the complexity of GPU algorithmic optimizations that are critical to high-performance writing operations, CODAG provides several major types of optimized writing primitives to support a wide range of popular encoding techniques.

### B. CODAG Meta-data and Performance APIs

CODAG provides an infrastructure for realizing the warp-level decompression as well as the optimized reading and writing operations to lower the programming effort when using CODAG for different encoding techniques. To isolate the complexity of GPU optimizations from decompressor developers, CODAG provides `input_stream` and `output_stream` abstractions that transparently manage the synchronization, coalescing and metadata for the on-demand reading and writing operations. Developers can simply call the member functions, shown in Table I and Table II, as needed to read and write data efficiently.

To support the highly efficient on-demand reading and writing operations, `input_stream` and `output_stream` internally manage meta-data such as offsets for the reading and writing pointers, information of input buffer, or fetched bites in the top entry of the input buffer. With these provided reading and writing primitives, CODAG only requires small changes to the sequential decoding code as the memory access optimizations are hidden via the internal functions. In the next few sections, we will discuss the CODAG decompression scheme and its optimizations more in detail.

### C. Warp Level Decompression

The large granularity of the decompression units in the state-of-the-art limits the scheduler’s ability to hide latency, because the vast majority of threads end up spending most

TABLE II: CODAG APIs for `output_stream`.

Member Functions	Description
<code>write_byte(int8_t b)</code>	Write a literal (byte) to the output buffer
<code>write_run(T init, size_t len, T delta)</code>	Write a run based on an initial value of type T, a length, and a delta.
<code>memcpy(int off, int len)</code>	Mempcy operation for dictionary-based encoding with the offset and length.

of their execution time waiting for a few leader threads to finish sequential decoding. The left side of Figure 4 is a cartoon illustration of how the instructions are issued during the decompression for the state-of-the-art decompressor. We assume an SM with two schedulers and an occupancy capacity of 4 warps for the example. In this tiny example, assume that the state-of-the-art has a decompression unit of a thread block that consists of two warps. Thus, only two independent compressed chunks (green and orange) can be assigned to a single SM in the state-of-the-art where one of the two warps is specialized to prefetch data from global memory into the buffers, and both warps work together to perform writes to global memory after the leader has decoded a symbol.

We assume that during the first part of the timeframe, each scheduler is issuing instructions of the warp containing the leader thread of one of the decompressor units and, for simplicity, that the batch buffer is full so there is no prefetch activity. Since there is effectively only one thread active in each scheduler, the latency of the function units is fully exposed, shown as pipeline bubbles between the decoding operations. After the decoding operations are complete, all threads synchronize, incurring the synchronization pipeline bubbles before the write operations. The SM execution resources are underutilized due to the pipeline bubbles.

The right side of Figure 4 shows the execution timing of CODAG. CODAG uses warps as a decompression unit to allow more chunks (green, orange, purple, blue) to be decompressed simultaneously. This gives the hardware scheduler more independent warps to work with. Assume that the green and purple warps are assigned to scheduler 1 whereas the orange and blue are assigned to scheduler 2. During the first part of the time frame, the decoding operations of the green and blue warps can be issued alternatively to tolerate each other’s latency. Thus, the SM execution resources are much better utilized. In reality, the reading, decoding, and writing operations of all the warps will be mixed together to more fully utilize the memory bandwidth than what is shown in Figure 4. That is, since there are no inter-warp dependencies in CODAG, the SM’s scheduler has a wider pool of useful instructions to schedule from and thus can better reduce pipeline bubbles and hide latencies. Furthermore, there is no more synchronization overhead before the writing operations.

#### D. CODAG Decoding Scheme

As the prefetch warp is removed in CODAG’s warp-level decompression scheme, all threads in the warp collectively execute on-demand reading operations during decoding whenever there are not enough fetched bytes. To do this, the decoding state needs to be saved before the reading operation

and restored after the reading operation to enable the leader thread to continue decoding after the reading operations.

To avoid the above-mentioned overhead during the transitions between the decoding operations and the reading/writing operations, CODAG uses an all-thread decoding technique by activating all threads in the warp to execute the same serial decoding operations on the same chunk. In this decoding scheme, all threads have a local copy of decoded information as they execute the same decoding process thus broadcasts are no longer needed. As for the reading operations, all threads in the warp only need to perform a low-cost warp-level synchronization to ensure a consistent view of the input buffer before reading as newer GPU architectures [20], [21] do not guarantee lock-step execution of the threads in a warp. After the reading operation, all threads in the warp can return naturally to continue the decoding operation, eliminating the need for explicitly saving and restoring the decoding state.

Since the decoding operation is redundantly performed by all threads in a warp, one might take a pessimistic view of the all-thread decoding technique. Thus, we use a micro-benchmark to compare the ALU compute throughput of the single-thread decoding and the all-thread decoding. For this micro-benchmark, the number of arithmetic operations executed per global memory access is varied from 1 to 100,000 to capture the compute throughput at different compute intensity levels. The result shows that the difference in compute throughput of the two decoding techniques never exceeds 0.1%. Thus, the additional arithmetic operations executed due to the all-thread decoding technique do not degrade the achieved compute throughput.

---

#### Algorithm 1 On-demand Reading With Shared Input Buffer

---

```

1: if len - counter < 128 then
2:   barrier()
3:   read_idx = offset + lane * 4
4:   enq_idx = (head + counter + lane) % len
5:   Buff[enq_idx] = Input[read_idx]
6:   counter += 128
7:   barrier()
8: end if
9: req_val = Buff[head]
10: head = (head + 1) % len
11: counter--
12: return req_val

```

---

#### E. Coalesced On-Demand Reading Operation

To maximize the benefits of the warp-level decompression scheme, CODAG also provides the APIs for highly efficient on-demand reading operations since it is also critical to maintain the coalesced access patterns in reading compressed data to optimize GPU memory bandwidth utilization. Thus, CODAG implements coalesced on-demand reading operations behind the `input_stream` abstraction.

CODAG’s on-demand reading operation with its default configuration is illustrated with the pseudocode in Algorithm 1. By default, CODAG deploys an input buffer in shared memory, to temporarily store the fetched bytes, minimizing the number of global memory accesses. The size of the input buffer is at least twice the cacheline size so that entire

cachelines can be easily enqueued in the input buffer. An input buffer also has a head pointer for threads to determine where to read from in the input buffer, and a length to keep track of the number of bytes left in the buffer.

For a given on-demand reading operation, all threads in a warp first collectively refill the shared input buffer with bytes fetched from a cacheline. Each thread in the warp fetches 4-bytes after a warp-synchronization barrier to ensure coalesced memory accesses. Once the input buffer is refilled, threads update the offset into the input in the `input_stream` instance. Then, the threads read the requested bits from the input buffer using the head pointer and update the internal state of its `input_stream` for the next on-demand reading operation.

**Using Registers:** The shared memory usage for the input buffer might limit the applicability of CODAG in applications with high shared memory utilization. To address this, CODAG provides a configuration where the input buffer is implemented with the threads’ local registers instead of the shared memory. In this configuration, each thread uses two 32-bits registers to implement the input buffer.

Similar to the default configuration, the input buffer is first refilled when there is enough space to store a complete cache-line. This is done by leveraging double buffering where two sets of 32 local registers across the warp operate as a double buffer. Since the data is stored in a local register, CODAG exploits warp-wise broadcast when fetching requested bytes from the input buffer. For this operation, the head pointer is first used to identify which thread’s local register is holding the requested bytes so that the requested bytes can be broadcast by the appropriate thread to all other threads in a warp.

### F. Coalesced On-demand Writing Operation

---

#### Algorithm 2 Memcpy(offset, len)

---

```

1: if lis_4B_aligned(write_ptr) then
2:   pad_bytes = (4 - (write_ptr % 4)) % 4
3:   byte_memcpy(offset, pad_bytes)
4: end if
5: barrier()
6: num_itr = ceil((len - pad_bytes) / 128)
7: for (int i = 0; i < num_itr; i++) do
8:   read_idx = ceil((read_ptr + lane*4) / 4)
9:   r1 = out[read_idx-1]
10:  r2 = out[read_idx]
11:  rdata = funnel_shift(r1, r2, read_ptr % 4)
12:  out[(write_ptr + 4*tid) / 4] = rdata
13:  read_ptr, write_ptr += 32
14:  barrier()
15: end for

```

---

Similar to the on-demand reading operations, CODAG supports highly efficient coalesced on-demand writing operations to reduce the cost of memory accesses. Ideally, all threads in a warp should collectively execute an on-demand writing operation of a full cacheline and then synchronize. However, as the required writing operations can vary based on the encoding techniques, CODAG provides optimized writing primitives to support the most common encoding techniques: 1) writing a literal value, 2) writing a run with delta (delta is 0 for a simple run), and 3) memory copy (memcpy).

**Writing a literal value:** As this operation only requires a few bytes to write to the output buffer, only one thread executes this operation.

**Writing a run:** This operation is commonly used for RLE-based encoding techniques. For this operation, each thread independently computes its decompressed value based on the initial value, delta, and thread index and then writes it to the output buffer at the appropriate offset to maximize memory utilization.

**Memcpy:** Common dictionary-based encoding techniques compress data with a length specifying the number of bytes to copy from the dictionary to the output buffer and an offset into the output buffer from the last byte written before the current memcpy starts. Unlike a regular memcpy, using a warp to perform a memcpy operation in a dictionary-based compression algorithm has a couple of challenges.

First, as the dictionary is implicit in the previously written output, the reading and the writing pointer both point to the same output buffer. Second, common algorithms only provide byte alignment for both the input and the output. These characteristics make it difficult to exploit the warp’s parallelism in memcpy, especially when we would like each thread to copy more than 1-byte (e.g. 4-bytes) at a time for better coalescing, reduced executed memory instructions, and improved GPU cacheline and memory bandwidth utilization.

To address these challenges, we design CODAG’s fast memcpy operation, shown in Algorithm 2. For a given memcpy operation, the threads first fetch the writing pointer from `output_stream` and check whether it is 4-byte aligned (line 1 in Algorithm 2). If it is not aligned, the threads collectively copy up to 3 bytes to guarantee 4-byte alignment (line 3). Once the writing pointer is aligned, the warp synchronizes to ensure that the copied bytes are visible to the whole warp. Then, the warp executes copy operation in iterations to cover the entire memcpy length, with each thread writing one 4-byte value to the output each iteration. Each thread independently calculates its reading pointer for a given iteration based on its warp lane index (line 8). Since the reading pointer is not guaranteed to be 4-byte aligned, each thread reads two consecutive 4-byte elements (line 9-10), then bit-shifts and concatenates them to generate the correct 4-byte output element (line 11) to write to its assigned offset (line 12).

Note, in each iteration, each thread in the warp independently reads two 4-byte elements written in previous iterations and writes one complete 4-byte element. We found that using 4-byte granularity for the memcpy loop body provided the best trade-off between overhead to align the writing pointer, the amount of parallelism exposed, and cacheline utilization. All threads in a warp synchronize at the end of each loop iteration, preventing race conditions between iterations.

Moreover, with dictionary compression, it is possible that the length of a memcpy is larger than the offset. In this special case, the byte sequence from the offset till the end of the output (before the memcpy executes) is to be appended to the output, possibly multiple times. Just like in Algorithm 2, we first align the writing pointer to 4-bytes and then assign

each thread one 4-byte output element to generate per memcpy loop iteration. However, in this special case, each 4-byte output element is created by combining two consecutive 4-byte elements in a fixed circular window of 4-byte elements, starting from the 4-byte element pointed to by the offset until the last 4-byte element of the output buffer. Thus, each thread can independently use modulo-arithmetic to find the two consecutive 4-byte elements in the specified window, and bit-shift and concatenate them to generate its output element each iteration. We don't show the algorithm listing for this case due to space constraints.

## V. EVALUATION

Our evaluation demonstrates that: (1) CODAG framework improves the performance of decompression by efficiently utilizing the hardware resources provided by the GPU. CODAG provides  $13.46\times$ ,  $5.69\times$ ,  $1.18\times$  decompression throughput speed up (geomean) on ORC RLE v1, ORC RLE v2, and Deflate compared to the state-of-the-art implementation in NVIDIA RAPIDS [1]. (2) A decompressor implemented in the CODAG framework can rival the state-of-the-art GPU implementation without application-specific optimizations.

### A. Experiment Setup

We evaluate CODAG using three different encoding techniques, namely RLE v1 and RLE v2 from the Apache ORC file format, and Deflate. These encoding schemes are chosen due to wide applicability but other encodings can also be enabled. We compare CODAG and the state-of-the-art NVIDIA RAPIDS baseline on an environment shown in Table III. We lock the GPU's clock frequency to peak before running the experiments.

### B. Evaluation Datasets

For each algorithm, we evaluate CODAG and the baseline on seven real-world sample datasets curated from four industrial application domains as shown in Table IV. Each dataset has unique properties enabling us to evaluate the proposed scheme on not only different types of encoding techniques but also different data types and patterns. For example, MC0 and MC3 have long run-lengths while TPC and TPT contains many repeated patterns. CD2, and TC2 follow power law distributions for the data. HRG is human genome dataset and has repeated text pattern containing A,T,C,G and N characters.

For the baseline, we use the official data management tools provided by ORC [2] to compress data with RLE v1 and RLE v2 algorithms. To compress the data with deflate, we use the zlib library [22] with a compression level of 9, the highest compression level. The chunk size for the original data is fixed to be 128KB for both CODAG and the baseline.

### C. Latency Analysis

To analyze how effectively CODAG hides latency and utilizes resources, we measured the stalled instruction distribution and compute/memory throughput percentages of CODAG and

TABLE III: Configuration used to evaluate CODAG.

Configuration	Specification
CPU	AMD EPYC 7702 64-Core Processor
Memory	1TB DDR4
GPU 1	NVIDIA Tesla V100 HBM2 32GB
GPU 2	NVIDIA A100 HBM2 40GB

TABLE IV: Real-world dataset used for evaluating CODAG.

Dataset	Category	DType	Size (GB)
Mortgage Col 0 (MC0) [23]	Analytics	uint_64	4.86
Mortgage Col 3 (MC3) [23]	Analytics	fp32	2.43
NYC Taxi Passenger Count (TPC) [11]	Analytics	int_8	3.07
NYC Taxi Payment Type (TPT) [11]	Analytics	char	7.41
Criteo Dense 2 (CD2) [17]	Recommenders	uint_32	0.73
Twitter COO Col 1 (TC2) [24]	Graph	uint_64	5.47
Human Reference Genome (HRG) [25]	Genomics	char	3.1

TABLE V: Compression Ratios and average compressed symbol length when the datasets are compressed by RLE v1, RLE v2, and Deflate. The compressed symbol length for RLE v2 is excluded due to various compressed types for RLE v2.

Dataset	Compression Ratio			Avg Comp Sym Len	
	RLE v1	RLE v2	Deflate	RLE v1	Deflate
MC0	0.023	0.022	0.017	29.7	81.3
MC3	0.038	0.039	0.015	40.5	156.6
TPC	0.867	0.637	0.119	1.00	10.1
TPT	1.41	0.99	0.042	1.00	32.6
CD2	0.286	0.308	0.625	20.9	5.89
TC2	0.087	0.075	0.0172	34.3	67.3
HRG	0.975	0.972	0.305	1.00	7.76

the baseline. For the stalled instruction distribution, we measured the number of instructions stalled due to synchronization (SB) and Math Pipeline Throttle (MPT). Measuring SB helps to understand thread occupancy during decompression, and measuring MPT helps us to understand the pressure on computing units as MPT means the instructions are stalled to wait on a specific oversubscribed math pipeline.

In this experiment, MC0 and TPC datasets are used for the measurement as they have drastically different compression ratios. As shown in Figure 5, we observe a dramatic difference in SB percentages between the baseline and CODAG. The lower SB percentage shows that there are more active threads during decompression. Moreover, we observe substantially more instructions are stalled due to MPT in CODAG, showing CODAG utilizes more compute resources and shifts decompression from latency-bound to compute-bound on GPUs.

Figure 6 shows that CODAG achieves a higher memory throughput percentage compared to the baseline. This is because CODAG optimally utilizes memory bandwidth by leveraging coalesced on-demand reading/writing operations and enabling more memory instructions to be executed in parallel by higher ILP.

### D. Decompression Throughput

We now evaluate the decompression throughput (output bytes per second) of CODAG and RAPIDS on three encoding techniques. Figure 7 shows the decompression throughput of

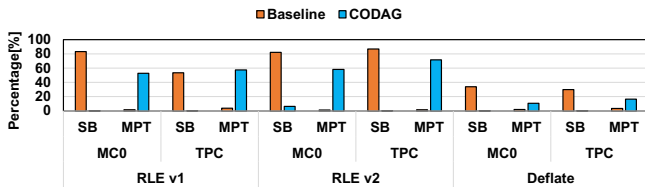


Fig. 5: Stalled instruction distribution comparison between CODAG and RAPIDS baseline.

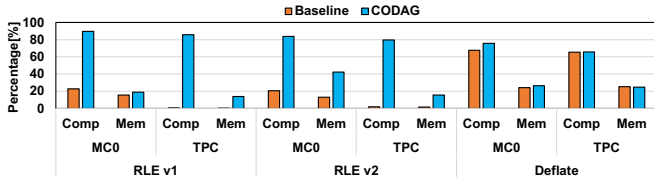


Fig. 6: Comparing the compute/memory peak throughput of CODAG and RAPIDS. Comp/Mem stand for compute/memory throughput percentage.

each encoding technique for both CODAG and the baseline, and Figure 8 shows the CODAG speedup over the baseline decompressor. As shown in Figure 7, CODAG achieves 38.07 GBps, 26.87 GBps, and 51.96 GBps geo-mean decompression throughput while the state-of-the-art decompressor achieves 2.83 GBps, 4.72 GBps, and 44.18 GBps. Thus, CODAG achieves 13.46 $\times$ , 5.69 $\times$ , and 1.18 $\times$  geo-mean speed ups compared to the baseline as shown in Figure 8.

CODAG sees significantly higher decompression throughput in MC0 and MC3 datasets. This is because highly compressible datasets amplify the effective memory bandwidth, requiring fewer bytes to decompress the chunk and enabling more active threads during writing operations. In our datasets, the mortgage datasets (MC0 and MC3) are highly compressible datasets, thus showing the highest decompression throughput.

We note that CODAG achieves substantially higher speedups over the baseline for RLE-based encoding techniques than Deflate. This is because with the state-of-the-art the average run length needs to be longer for RLE v1 for best thread occupancy; else, most threads become inactive during writing operations.

#### E. Single-Thread Decoding vs All-Thread Decoding

Next, we present the benefit of performing all-thread decoding over single-thread decoding for RLE v1 (RLE v2 has similar behavior) and Deflate decompression. When we compare the decompression throughput of the two decoding techniques, the result shows the CODAG with the all-thread decoding technique achieves 1.17 $\times$  and 1.19 $\times$  higher geo-mean decompression throughput than the single-thread decoding technique. As discussed in § IV-D, this shows CODAG successfully reduces the number of broadcast operations while maintaining the achieved compute throughput of ALUs.

#### F. Impact of Finer Decompression Unit

This section presents an ablation study to show that (1) reducing the number of threads responsible for decoding a chunk is key to CODAG’s performance gains, and (2) CODAG’s

warp-level decompression, i.e., without a prefetching warp, further improves performance.

For this evaluation, we add a prefetch warp to CODAG, such that two warps are scheduled per chunk - one warp to prefetch compressed input data and one warp to perform the decompression. This makes the CODAG architecture more similar to the baseline except that the baseline allocates more threads to decompress each chunk - 1024 threads for RLE v1 and RLE v2 and 128 threads for Deflate.

Figure 8 shows CODAG with a prefetching warp is able to achieve 7.10 $\times$ , 4.33 $\times$ , and 1.02 $\times$  higher geo-mean decompression throughputs compared to the baseline for the three respective encoding techniques. Based on the result, finer decompression units enable the GPU hardware to tolerate compute operation and memory latency more effectively.

However, the performance gains for each of the three encoding techniques is lower than the performance gains achieved by CODAG’s single-warp decompression unit, i.e. without a prefetching warp. This is because the decompression process is not bounded by memory bandwidth, thus manually allocated hardware resources for prefetching to tolerate memory latency limits hardware resource utilization. Additionally, CODAG minimizes the cost of memory access latency by coalesced on-demand memory operations. Thus, the benefits from re-allocating the resources used for prefetching to decoding out-scales the benefits from prefetching units.

#### G. Impact of Hardware Resources

In the previous sections, we establish that CODAG offers superior decompression bandwidth on A100 GPU compared to the baseline. In this section, we constrain the CODAG and baseline design by downgrading the GPU to NVIDIA Volta V100. From this experiment, we analyze the impact of hardware resources on CODAG and the scalability of CODAG and the baseline design.

As shown in Figure 8, CODAG achieves 11.19 $\times$ , 4.39 $\times$ , and 1.10 $\times$  geo-mean speed up compared to the baseline on V100 while it achieves 13.46 $\times$ , 5.69 $\times$ , and 1.18 $\times$  geo-mean speed up compared to the baseline on A100. The impact of compute under-utilization becomes more critical as newer GPU provides higher compute resources and memory bandwidth. Thus, we observe CODAG scales better than the baseline with the available hardware resources as it more efficiently exploits parallelism provided by the GPUs.

## VI. RELATED WORK

**Parallel compression/decompression with CPUs:** Multiple efforts to parallelize compression and decompression algorithms on CPUs have been proposed in the past [26]–[28]. pigz decompression is inherently hard to parallelize due to data dependency between the variable-length compressed blocks [26], [29]. Zstd [28] and pbzip2 [27] implementations add decompressed size as part of their headers to exploit parallelism. However, such coarse-grain parallelism across the compressed blocks is insufficient to fully utilize GPUs [13].

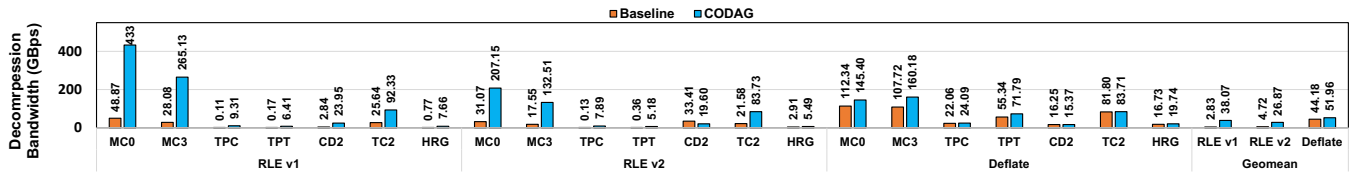


Fig. 7: Comparing decompression throughput of CODAG and RAPIDS baseline on A100 GPU.

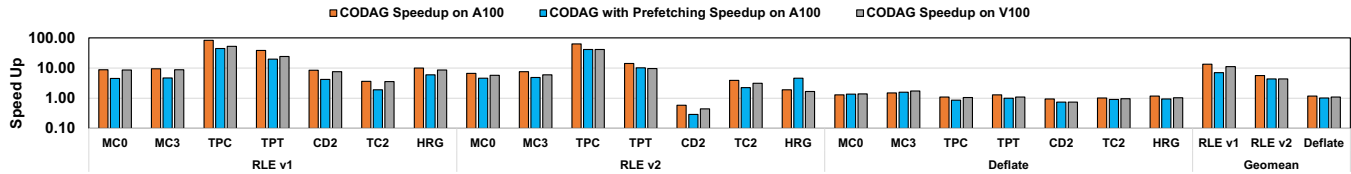


Fig. 8: CODAG speedup without and with a prefetching warp when compared to RAPIDS in the latest two generations of NVIDIA GPUs. First two bars represent the speedup compared to RAPIDS on A100, and the baseline for the third bar is RAPIDS on V100.

**GPU Decompression:** Several prior works have proposed implementing efficient compression or encoding algorithms for GPUs [4], [12]–[14], [30]–[35]. The prior works [12]–[14], [30], [33], define their own file formats to achieve high decompression throughput for Deflate algorithm on GPU and propose to split the input data into smaller data blocks. However, compared to CODAG, the datasets should go through expensive pre-processing steps to recompress the entire datasets into their own data format. Other prior works [31], [32], [34], [35] leverage algorithm-specific optimizations, limiting flexibility.

## VII. CONCLUSION

In this work, we introduced CODAG, a flexible framework for high throughput decompression on GPUs without requiring decompressor developers to implement sophisticated, GPU-specific optimizations. CODAG exploits warp-level decompression and highly efficient on-demand reading and writing operations to effectively hide latencies. Moreover, CODAG completely removes the broadcast operations by dedicating all threads to participate in decoding. Our evaluations show that CODAG can achieve 13.46 $\times$ , 5.69 $\times$ , and 1.18 $\times$  speed up compared to the state-of-the-art decompressor for RLE v1, RLE v2, and Deflate encoding techniques.

## REFERENCES

- [1] “CUDA RAPIDS: GPU-Accelerated Data Analytics and Machine Learning,” <https://developer.nvidia.com/rapids>, 2020.
- [2] A. S. Foundation, “Orc file format specification,” <https://orc.apache.org/specification/>, 2021.
- [3] W. McKinney and the Pandas Development Team, “pandas: powerful python data analysis toolkit,” <https://pandas.pydata.org/docs/>, 2022.
- [4] “A library for fast lossless compression/decompression on the gpu,” <https://github.com/NVIDIA/nvcomp>, 2020.
- [5] “Accelerating Lossless GPU Compression with New Flexible Interfaces in NVIDIA nvCOMP,” <https://developer.nvidia.com/blog/accelerating-lossless-gpu-compression-with-new-flexible-interfaces-in-nvidia-nvcomp/>, 2022.
- [6] “Boosting Data Ingest Throughput with GPUDirect Storage and RAPIDS cudFP,” <https://developer.nvidia.com/blog/boosting-data-ingest-throughput-with-gpudirect-storage-and-rapids-cudfp/>, 2022.
- [7] D. Wang, F. Zhang, W. Wan, H. Li, and X. Du, “Finequery: Fine-grained query processing on cpu-gpu integrated architectures,” in *2021 IEEE International Conference on Cluster Computing (CLUSTER)*, 2021, pp. 355–365.
- [8] S. Floratos, M. Xiao, H. Wang, C. Guo, Y. Yuan, R. Lee, and X. Zhang, “Nestgpu: Nested query processing on gpu,” in *2021 IEEE 37th International Conference on Data Engineering (ICDE)*, 2021, pp. 1008–1019.
- [9] Y. Liu, J. Wang, and S. Swanson, “Griffin: Uniting cpu and gpu in information retrieval systems for intra-query parallelism,” *SIGPLAN Not.*, vol. 53, no. 1, p. 327–337, feb 2018. [Online]. Available: <https://doi.org/10.1145/3200691.3178512>
- [10] J. Li, H.-W. Tseng, C. Lin, Y. Papakonstantinou, and S. Swanson, “HipgriffinDB: Balancing I/O and GPU Bandwidth in Big Data Analytics,” *Proceedings of the VLDB Endowment*, vol. 9, no. 14, p. 1647–1658, Oct. 2016.
- [11] The City of New York, “TLC Trip Record Data,” <https://www1.nyc.gov/site/tlc/about/tlc-trip-record-data.page>.
- [12] S. Funasaka, K. Nakano, and Y. Ito, “Adaptive loss-less data compression method optimized for gpu decompression,” *Concurrency and Computation: Practice and Experience*, vol. 29, no. 24, p. e4283, 2017.
- [13] E. Sitaridi, R. Mueller, T. Kaldewey, G. Lohman, and K. A. Ross, “Massively-parallel lossless data decompression,” in *2016 45th International Conference on Parallel Processing (ICPP)*, 2016, pp. 242–247.
- [14] A. Shanbhag and B. W. Yogatama, “Tile-based lightweight integer compression in gpu,” *Proceedings of the 2022 International Conference on Management of Data*, pp. 1390–1403, 2022.
- [15] Z. Qureshi, V. S. Malthody, I. Gelado, S. W. Min, A. Masood, J. Park, J. Xiong, C. Newburn, D. Vainbrand, I.-H. Chung, M. Garland, W. Dally, and W. mei Hwu, “Bam: A case for enabling fine-grain high throughput gpu-orchestrated access to storage,” 2022.
- [16] A. S. Foundation, “Parquet file format specification,” <https://parquet.apache.org/docs/file-format/>, 2022.
- [17] Criteo AI Lab, “Criteo 1TB Click Logs dataset,” <https://ailab.criteo.com/download-criteo-1tb-click-logs-dataset/>.
- [18] P. Deutsch, “Rfc8478: Zstandard compression and the application/zstd media type,” <https://tools.ietf.org/html/rfc1951>, 1996.
- [19] D. A. Huffman, “A method for the construction of minimum-redundancy codes,” *Proceedings of the IRE*, vol. 40, no. 9, pp. 1098–1101, 1952.
- [20] “NVIDIA Tesla V100 GPU Architecture Whitepaper,” <https://images.nvidia.com/content/volta-architecture/pdf/volta-architecture-whitepaper.pdf>, 2017.
- [21] “NVIDIA Tesla A100 Tensor Core GPU Architecture,” <https://www.nvidia.com/content/dam/en-zz/Solutions/Data-Center/nvidia-ampere-architecture-whitepaper.pdf>, 2020.
- [22] J. G. G. Roelofs and M. Adler, “A massively spiffy yet delicately unobtrusive compression library,” <https://www.zlib.net/>, 2022.
- [23] F. Mae, “Fannie mae single-family loan performance data,” <https://docs.rapids.ai/datasets/mortgage-data>.
- [24] H. Kwak, C. Lee, H. Park, and S. Moon, “What is Twitter, a Social Network or a News Media?” in *Proceedings of the 19th International Conference on World Wide Web*, ser. WWW ’10, Raleigh, NC, 2010.
- [25] N. C. for Biotechnology Information, “Human reference genome (grch38-fasta),” <https://www.ncbi.nlm.nih.gov/genome/guide/human/>.
- [26] M. Adler, “Parallel gzip,” <https://zlib.net/pigz/>, 2010.
- [27] J. Gilchrist, “Parallel bzip2 file compressor,” <https://linux.die.net/man/1/pbzip2>, 2015.

- [28] Y. Collet and M. Kucherawy, "Rfc8478: Zstandard compression and the application/zstd media type," <https://tools.ietf.org/html/rfc8478> and <https://facebook.github.io/zstd/>, 2015.
- [29] H. Jang, C. Kim, and J. W. Lee, "Practical speculative parallelization of variable-length decompression algorithms," in *Proceedings of the 14th ACM SIGPLAN/SIGBED Conference on Languages, Compilers and Tools for Embedded Systems*, ser. LCTES '13. New York, NY, USA: Association for Computing Machinery, 2013, p. 55–64.
- [30] T. Lloyd, K. Barton, E. Tiotto, and J. N. Amaral, "Run-length base-delta encoding for high-speed compression," in *Proceedings of the 47th International Conference on Parallel Processing Companion*, ser. ICPP '18. New York, NY, USA: Association for Computing Machinery, 2018.
- [31] R. A. Patel, Y. Zhang, J. Mak, A. Davidson, and J. D. Owens, "Parallel lossless data compression on the gpu," in *2012 Innovative Parallel Computing (InPar)*, 2012, pp. 1–9.
- [32] A. Ozsoy, M. Swany, and A. Chauhan, "Optimizing lzss compression on gpgpus," *Future Generation Computer Systems*, vol. 30, pp. 170 – 178, 2014.
- [33] M. A. O'Neil and M. Burtscher, "Floating-point data compression at 75 gb/s on a gpu," in *Proceedings of the Fourth Workshop on General Purpose Processing on Graphics Processing Units*, ser. GPGPU-4. New York, NY, USA: Association for Computing Machinery, 2011.
- [34] A. Ozsoy, M. Swany, and A. Chauhan, "Pipelined parallel lzss for streaming data compression on gpgpus," in *2012 IEEE 18th International Conference on Parallel and Distributed Systems*, 2012, pp. 37–44.
- [35] M. Olano, D. Baker, W. Griffin, and J. Barczak, "Variable bit rate gpu texture decompression," in *Proceedings of the Twenty-Second Eurographics Conference on Rendering*, ser. EGSR '11. Goslar, DEU: Eurographics Association, 2011, p. 1299–1308.